Received: 8 February 2022 | Revised: 19 May 2022 | Accepted: 23 May 2022

DOI: 10.1096/fba.2022-00017

FASEB BioAdvances WILEY

RESEARCH ARTICLE

A novel fatty acid metabolism-related gene signature predicts the prognosis, tumor immune properties, and immunotherapy response of colon adenocarcinoma patients

Le Liu[1] | **Liping Liang**[2] | **Genghui Mai**[2] | **Ye Chen**[1,2]

[1]Department of Gastroenterology, Integrated Clinical Microecology Center, Shenzhen Hospital, Southern Medical University, Shenzhen, China

[2]Department of Gastroenterology, State Key Laboratory of Organ Failure Research, Guangdong Provincial Key Laboratory of Gastroenterology, Nanfang Hospital, Southern Medical University, Guangzhou, China

Correspondence
Ye Chen and Le Liu, Department of Gastroenterology, Integrated Clinical Microecology Center, Shenzhen Hospital, Southern Medical University, 1333 New Lake Road, Shenzhen 518100, China.
Email: yechen_fimmu@163.com (Y. C.) and 13246837972@163.com (L. L.)

Funding information
Postdoctoral Research Foundation of China, Grant/Award Number: 2021 M700065; National Natural Science Foundation of China, Grant/Award Number: 81900470 and 81770529

Abstract

Colon adenocarcinoma (COAD) has a high incidence and death rate. Despite the fact that change in fatty acid metabolism promotes tumor growth and metastasis to the greatest degree among metabolite profiles, a thorough investigation on the involvement of fatty acid metabolism-related genes (FAMRGs) in COAD has yet not been conducted. Here, the clinical data as well as the gene expression profiles were extracted from The Cancer Genome Atlas (TCGA) database. Based on the FAMRG expression data and clinical information, a FAMRG risk signature was developed using LASSO as well as multivariate and univariate Cox regression analyses. Then, the nomogram was used to create a customized prognostic prediction model, and the calibration and receiver operating characteristic curves were used to evaluate the nomogram's prediction performance and discriminative capability. Lastly, a number of studies were conducted to assess the influence of independent FAMRGs on COAD, including unsupervised cluster analysis, functional analysis, and drug sensitivity analysis. Three hundred and sixty-seven patients were included in this study, and a 12-FAMRG risk signature was discovered in the training cohort based on a detailed examination of the FAMRGs expression data and clinical information. After that, risk scores were computed to classify patients into low or high-risk groups, and the Kaplan–Meier curve analysis revealed that patients in the low-risk group exhibited an elevated overall survival (OS) rate. The FAMRG was shown to be substantially correlated with prognosis in multivariate Cox regression analysis and was validated using the validation dataset. Then, using the clinical variables and risk signature, we developed and validated a prediction nomogram for OS. Functional characterization showed a strong correlation between this signature and immune cell infiltration and immune modulation. Additionally, by evaluating the GDSC database, it was determined that the high-risk group exhibited medication resistance to many

Le Liu and Liping Liang contributed equally to this article.

chemotherapeutic and targeted medicines, including VX.680, gemcitabine, doxorubicin, and paclitaxel. Overall, we have revealed the significance of a FAMRG risk signature for predicting the prognosis and response to immunotherapy in COAD, and our findings might contribute to an enhanced comprehension of metabolic pathways and the future development of innovative COAD therapeutic methods.

KEYWORDS

colon adenocarcinoma, fatty acid metabolism, nomogram, prognostic prediction, tumor immune microenvironment

1 | INTRODUCTION

With a high incidence rate, colon adenocarcinoma (COAD) is the fourth major contributor to cancer-related death across the world.[1] Although progress has been made in diagnosing and treating COAD, mortality is still considerably high owing to the absence of markers for early detection and prognostic prediction.[2] The gold standard for the treatment of COAD is radical resection. However, it has been observed that the rate of recurrence of COAD is significant (almost 50%) within 2 years following radical resection, with 50% of the recurrences being deadly. Immunotherapy, particularly suppressors of immunological checkpoints such as programmed cell death 1 ligand 1 (PD-L1), programmed cell death protein 1 (PD-1), and cytotoxic T-lymphocyte antigen-4 (CTLA4), has given potential new options for improving the overall survival (OS) of COAD patients.[3,4] In recent years, pembrolizumab (an anti-PD-1 monoclonal antibody) was proven to have increased effectiveness and long-term therapeutic benefit in a subset of patients with COAD who had DNA mismatch repair-deficient (dMMR)/microsatellite instability-high (MSI-H).[5] Nonetheless, since the clinical effectiveness of these immune checkpoint inhibitors has only been shown in a limited number of COAD patients, it is very important to identify efficient prognostic indicators and additional immune checkpoint targets.

The tumor microenvironment (TME) is hypoxic and acidic with nutritional shortage, causing tumor cells and the surrounding stromal cells to exhibit abnormal metabolism.[6] Reprogramming the energy metabolism of tumors may enhance their fast growth, metastasis, proliferation, and survival, and is a newly recognized characteristic of cancer.[7,8] As previously stated, cancer cells are sensitive to the "Warburg effect", which is characterized by increased glycolysis or aerobic glycolysis.[9] Along with aberrant glucose metabolism, dysregulation of lipid metabolism has received increased emphasis in the past few decades as a hallmark of metabolic reprogramming in cancer, particularly COAD.[10] The disruption of lipid metabolism, specifically for fatty acid metabolism with altered expression and activity of lipid-metabolizing enzymes as a result of abnormal activation of oncogenic signaling pathways, has been widely recognized as a critical factor of metabolic reconfiguration within cancer cells and immune cells that may lead to the long-term development of COAD.[11] Furthermore, data acquired from several solid tumors shows that tumor immunometabolic reprogramming is highly essential, which will continue to be a new emphasis of COAD research in the future.[12–14] Fatty acids are essential for energy storage, membrane synthesis, and signaling molecule production during oncogenesis.[15] It has been shown that decoding the molecular mechanism of COAD and fatty acid metabolism might aid in the identification of new therapeutic targets and the development of successful treatment techniques. Wang et al. discovered that activating fatty acid oxidation through CPT1A reduces anoikis in COAD cells, suggesting that CPT1A is a promising target for metastatic COAD therapy.[16] Nonetheless, the regulation mechanism modulating the fatty acid metabolism route in COAD is yet not to be fully explored. As a result, identifying fatty acid metabolism-related genes (FAMRGs) may open up new options for investigating COAD therapy.

Our research aimed to establish a model to predict prognosis and direct therapeutic treatment in COAD patients by classifying them according to their fatty acid metabolism genes. We discovered two groups associated with fatty acid metabolism after classifying 367 COAD patients according to genes involved in fatty acid metabolism. The risk score may then be computed by building a model related to fatty acid metabolism using the LASSO-Cox approach. This risk score may be utilized in anticipating prognosis and immune infiltration. Our findings indicate a probable relationship between fatty acid metabolism, prognosis, and the immune microenvironment of COAD patients.

2 | MATERIALS AND METHODS

2.1 | Data collection

In order to obtain the RNA-seq read count and the associated clinical information, we used the The Cancer Genome Atlas (TCGA) database (available at https://portal.gdc.cancer.gov). To guarantee the better quality of the analysis, samples having a survival duration of ≥30 days were utilized. In addition, 367 COAD patients from the TCGA were enrolled for further investigation. Clinical information for COAD patients is presented in Table 1.

2.2 | Construction of training set and testing set and establishment of differentially expressed FAMRGs

We utilized the limma R program to evaluate the differentially expressed genes (DEGs) in the TCGA dataset in tumor and normal specimens in order to identify the differentially expressed FAMRGs (DE FAMRGs) related to COAD prognosis. A similar approach was utilized to detect the FAMRGs that were differentially expressed between the groups. For the following analyses, we selected the DEGs and FAMRGs with an adjusted $p < 0.05$ and an absolute log2-fold change (FC) >1. We found the DE FAMRGs at the points where the DEGs and the FAMRG lists intersect. Owing to the low amount of normal colon tissue samples available in the TCGA repository, we divided the dataset into training and testing sets at random using a ratio of (2:1). The training set was utilized to build a possible prognostic signature and the testing set was utilized to validate the signature.

2.3 | Weighted gene co-expression network analysis

FAMRGs were used to generate a weight co-expression network using the R package "WGCNA".[17] Clustering was performed using the topological overlap measure (TOM), and gene modules were found. We evaluated each module eigengene (ME), obtaining the expression level of each module. The cutoff value was set at $p < 0.05$.

2.4 | Consensus clustering

Consensus clustering utilizing k-means algorithms was conducted to identify novel fatty acid metabolism-related patterns associated with gene expression (Algorithm AS 136: a K-means clustering algorithm). The stability and number of clusters were determined utilizing the consensus clustering approach implemented in the "ConsensuClusterPlus" package. To confirm the stability of our clusters, we repeated the above approach 1000

TABLE 1 Baseline characteristics of patients with COAD in TCGA database

Covariates	Type	Total ($n = 367$)	Test	Train	p-value
Age	<=65	150 (40.87%)	43 (35.54%)	107 (43.5%)	0.1786
	>65	217 (59.13%)	78 (64.46%)	139 (56.5%)	
Gender	Female	174 (47.41%)	56 (46.28%)	118 (47.97%)	0.847
	Male	193 (52.59%)	65 (53.72%)	128 (52.03%)	
Stage	Stage I	64 (17.44%)	24 (19.83%)	40 (16.26%)	0.0973
	Stage II	148 (40.33%)	56 (46.28%)	92 (37.4%)	
	Stage III	102 (27.79%)	24 (19.83%)	78 (31.71%)	
	Stage IV	53 (14.44%)	17 (14.05%)	36 (14.63%)	
T	T1	8 (2.18%)	1 (0.83%)	7 (2.85%)	0.3974
	T2	64 (17.44%)	25 (20.66%)	39 (15.85%)	
	T3	253 (68.94%)	83 (68.6%)	170 (69.11%)	
	T4	42 (11.44%)	12 (9.92%)	30 (12.2%)	
M	M0	278 (75.75%)	95 (78.51%)	183 (74.39%)	0.5391
	M1	53 (14.44%)	17 (14.05%)	36 (14.63%)	
	Unknown	36 (9.81%)	9 (7.44%)	27 (10.98%)	
N	N0	219 (59.67%)	82 (67.77%)	137 (55.69%)	0.0837
	N1	85 (23.16%)	23 (19.01%)	62 (25.2%)	
	N2	63 (17.17%)	16 (13.22%)	47 (19.11%)	

times [ConsensusClusterPlus: a class finding tool with confidence evaluation and item tracking].

2.5 | Constructing and validating the prognostic signature

COAD patients were classified into training and test cohorts according to the 2:1 ratio at random. An investigation into the link between each training cohort's FAMRG expression and OS was conducted using a single-variable Cox regression analysis. Then, using the R package "glmnet," these FAMRGs were re-examined using LASSO penalized Cox proportional hazards regression in order to pick the most accurate risk model. In order to determine the risk score for each patient, the equation below was utilized: risk score = $(h_0t)\sum (coef_i * Exp_i)$, where $coef_i$ denotes the coefficient of each FAMRG, Exp_i denotes each FAMRG expression value, and h_0t indicates the baseline hazard function. The patients were divided into two risk groups based on the median risk score. Furthermore, the Kaplan–Meier techniques from the R survminer package were utilized to create the survival curve, and the differences between the two risk groups were determined using the log-rank test. In the meantime, the R package "survivalROC" was utilized to create a time-dependent receiver operating characteristic (ROC) curve and the area under the curve (AUC) was obtained to examine the accuracy of the prognostic risk signature. To validate the prediction ability of the prognostic signature, risk scores were computed in the testing cohort using the similar aforementioned prognostic equation, and Kaplan–Meier survival and ROC curve analyses were performed utilizing the median risk score as the cutoff value.

2.6 | Independence of the FAMRGs signature

By using the FAMRG features of OS and relevant clinical information, we utilized univariate Cox regression analysis to assess independence. The statistical significance threshold was set at $p < 0.05$.

2.7 | Constructing and validating the nomogram

The column line diagram works by creating a multifactor regression model (Cox regression, logistic regression, etc.), scoring each influencing factor's contribution to the model's outcome variable (the magnitude of the regression coefficient), adding the individual scores to get the total score, and finally calculating the predicted value. All independent prognostic factors were assessed by multivariate Cox regression analysis after being identified through univariate Cox regression analysis. Then, the "rms" R package (https://cran.r-project.org/web/packages/rms/index.html) was utilized to construct the nomogram on the basis of all filtered prognostic indicators. Subsequently, we evaluated the discrimination of the nomogram, and the calibration plot curve analysis was performed.

2.8 | Gene set variation analysis (GSVA)

The "GSVA" R package was utilized to conduct GSVA on the gene profiles to assess the differences in biological processes between groups with high- and low-risk scores. GSVA, which is an unsupervised and nonparametric approach, can be used to determine the variations in pathways or biological processes based on an expression matrix sample. The reference gene set was derived from the "c2.cp.kegg.v7.1.symbols" gene sets in the molecular signatures database (https://www.gsea-msigdb.org/gsea/msigdb). A threshold of FDR <0.05 showed an enrichment pathway that was statistically significant.

2.9 | Gene set enrichment analysis (GSEA)

The pathway research began with a differential expression analysis of all genes to identify samples with high- or low-risk scores using the R software "DESeq2". It was decided to employ the GSEA technique, which was founded on the HALLMARK gene sets, in conjunction with the R-based "clusterProfiler" tool to find the signaling pathways that the DEGs are engaged in. It was determined that the pathways were statistically significant when FDR <0.05 and $p < 0.05$ were both met.

2.10 | Tumor microenvironment (TME) analysis

To investigate the TME in COAD, we used the CIBERSORT technique to calculate the amounts of infiltration of 22 different types of immune cells based on all genes' expression levels. We begin by uploading all gene expression data to the CIBERSORTx online portal. Following that, the LM22 signature was used to execute the algorithm for 1000 permutations. Further analysis was performed on COAD specimens with an output p-value <0.05. Additionally, the stromal and immunological scores were determined using the R package "estimate". Single sample GSEA (ssGSEA) analysis

was subsequently conducted to estimate the abundance of 28 immune infiltration cells using the R package "GSVA". Additionally, the TIMER 2.0 (Tumor Immune Estimation Resource) database was used to look into the association between mutant genes and COAD immune infiltration levels.

2.11 | Therapeutic sensitivity with prognostic signature

Subsequently, data on the gene bulk expression profiles of cancer cell lines and drug responsiveness (as determined by IC50 value) were obtained from the Genomics of Drug Sensitivity in Cancer (GDSC) database. GDSC has the most comprehensive collection of publicly available information on cancer cells' drug sensitivity and molecular indicators of therapeutic response.[18] Then, we used the LIBSVM program in R to estimate the IC50 value for each medication using default settings and a linear kernel. Finally, we compared the medication sensitivities of high- and low-risk groups to see if there were any differences.

2.12 | Statistical analysis

Statistical analyses on the data were carried out using the R programming language (version 4.0.4) and the R package. Wilcoxon test (Mann–Whitney test) was employed to evaluate continuous variables, while chi-square or Fisher's exact was employed to assess categorical variables. K-M and log-rank tests were used to find the difference in survival. $p < 0.05$ was set for all of the statistics that were done.

3 | RESULTS

3.1 | Acquisition of data

We obtained transcriptome information from the TCGA database for 398 colon cancer tissues and 39 paraneoplastic tissues. Three hundred and sixty-seven patients with complete follow-up time and clinical information were added to the study (baseline information). The Genecards database was used to identify fatty acid-related genes and GIFtS >30 and Score > 10 were the inclusion criteria, and 886 genes were finally included.

3.2 | Identification of disease subtypes

WGCNA suggested that the blue module genes were most significantly associated with colon cancer (cor = −0.87), and in order to reveal the correlation between fatty acid-related genes expression levels and COAD prognosis, we clustered the tumor sample using the "Consensus Cluster Plus" program based on the genes in the blue module (Figure 1A,B). We identified two COAD subtypes (Figure 1C–F). The Kaplan–Meier survival analysis illustrated that COAD patients in the C1 group exhibited a more favorable prognosis (Figure 2A,B). Results from the Estimate algorithm indicated that the stromal and ESTIMATE scores were greater in the C2 group (Figure 2C). The MCP-Counter score indicated that the C1 group had a greater T-cell count, while the monocytes, endothelial cells, and fibroblasts were elevated in the C2 group (Figure 2D–G). In addition, differential gene expression analysis suggested that there were a large number of differential genes between C1 and C2 groups, and there were significant differences in STAGE staging, TNM staging (Figure 2H). GSVA suggested that there were differences in many sets of pathways between C1 and C2 groups, especially containing fatty acid metabolic pathways (Figure 2I). This implies that the genes in the blue module are of great exploration value. Overall, our results suggest that COAD grouping is feasible.

3.3 | Construction and evaluation of the prognostic model

TCGA-COAD patients were classified at random into training and test groups in a 2:1 ratio. Univariate Cox regression was utilized to detect 15 prognosis-related genes in the training dataset using the genes in the blue module (Figure 3A). Twelve key FAMRGs were further screened out utilizing LASSO-Cox regression analysis (Figure 3B). The coefficient of each FAMRG was calculated to build a risk score model (Figure 3C). We utilized the median risk score as the threshold and allocated 367 patients into two groups: high- and low-risk groups. Low-risk patients had a significantly longer OS than those in the high-risk group, according to Kaplan–Meier curves (Figure 3D–F). The AUCs of 1-, 3-, and 5-year OS anticipated by the model were 0.813, 0.691, and 0.795, respectively, validating the prediction ability of the signature with satisfactory specificity and sensitivity (Figure 3G–I). The PCA suggested a high degree of discrimination between the low- and high-risk groups. We obtained similar outcomes using the same method for the test dataset (Figure 3J–L). A univariate Cox regression revealed that risk score and clinical features such as TNM staging and age were strongly associated with OS, and we then performed a multifactorial Cox analysis and discovered that 12-FAMRG signature was an independent prognostic marker for COAD ($p < 0.001$), implying that our signature could be a good complement

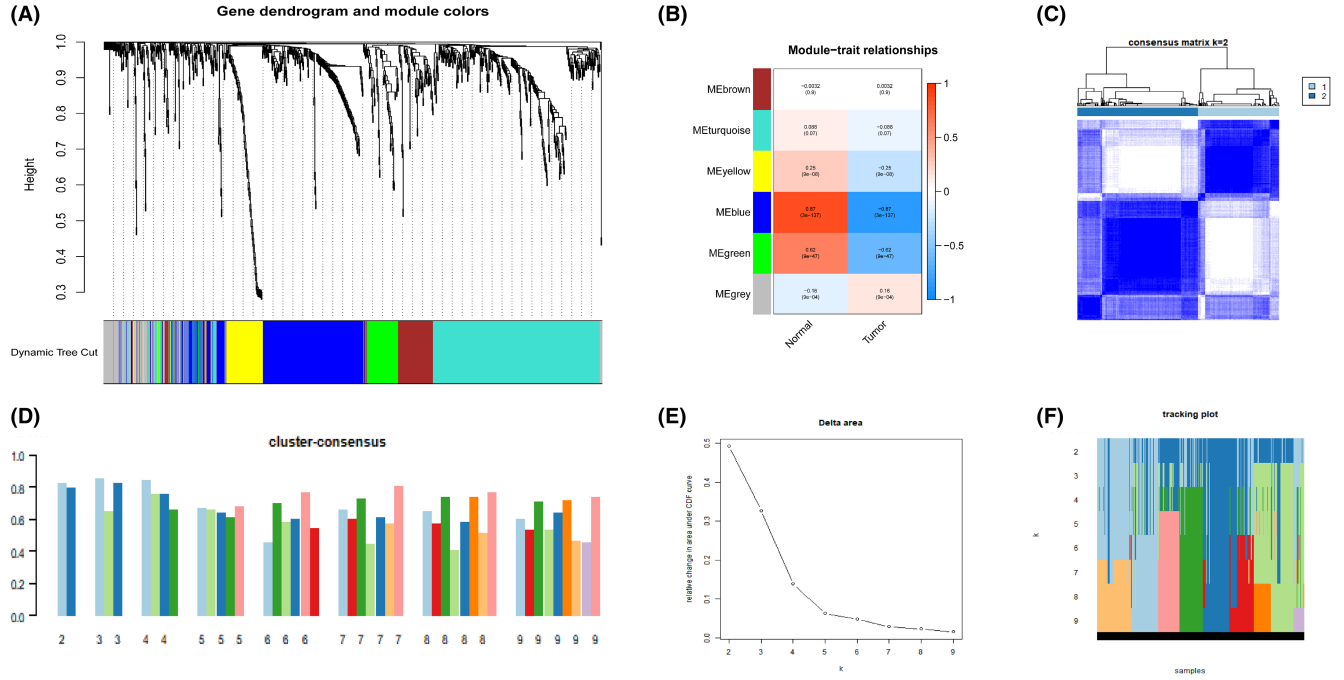

FIGURE 1 Weighted gene co-expression analysis and subgroups of COAD defined by the most significant FAMRGs filtered by WGCNA. (A) A dendrogram of gene clusters was created, with each cluster being represented by a different color. (B) Correlation analysis between gene cluster profiles and COAD. *p*-value and Pearson coefficient are denoted by the numbers within and outside the brackets, respectively. (C–F) Consensus score matrix for the TCGA cohort when K = 2. Two samples had a higher likelihood of clustering together if they exhibited a higher consensus score in separate interactions.

to conventional pathological staging (Figure 4A,B). After that, we developed a nomogram that included information such as STAGE staging, age, and risk score (Figure 5A). For 1-, 3-, and 5-year OS, the projected AUCs were 0.774, 0.791, and 0.765, correspondingly (Figure 5B). The prediction model's calibration curves and ROC findings jointly revealed that the model performed better in terms of prediction (Figure 5C–E).

3.4 | Relativity between risk score and clinicopathological features

A risk score difference analysis was performed to thoroughly investigate the correlation between clinical variables and the risk scores. The findings indicated that risk scores had greater value in the age over 65 years group. In addition, as the STAGE staging increased, the risk scores of patients were also greater. Consistent results were also obtained in TNM staging (Figure 6A–E).

3.5 | Molecular characteristics of the prognostic signature

GSEA was conducted on the low- and high-risk groups to clarify the potential biological mechanisms and signaling pathways correlated with risk scores. The DEGs in the high-risk group were largely abundant in cancer and tumor metastasis-related pathways, according to the data, including allograft rejection, epithelial-mesenchymal transition, aptical_junction, inflammatory response, interferon_gamma_response, ECM receptor, cytokine receptor, and focal adhesion signaling pathways (Figure 7A,C). The DEGs in the low-risk group, on the other hand, were primarily predominant in metabolic response-related pathways, including fatty acid metabolism and oxidative phosphorylation signaling (Figure 7B,D).

3.6 | Association between risk score and immune infiltration features

To identify the value of the TME of this signature, we differentially analyzed the tumor purity, and the stromal, immune, and ESTIMATE scores between the high-risk and low-risk groups. The outcomes illustrated that in the low-risk group, stromal score, immune score, and ESTIMATE score were elevated while the tumor purity was reduced, indicating a presence of more immune components in TME in this group (Figure 8A–D). Moreover, the risk score was positively associated with the stromal, immune, and ESTIMATE scores, and negatively associated with the tumor purity (Figure 8E–H).

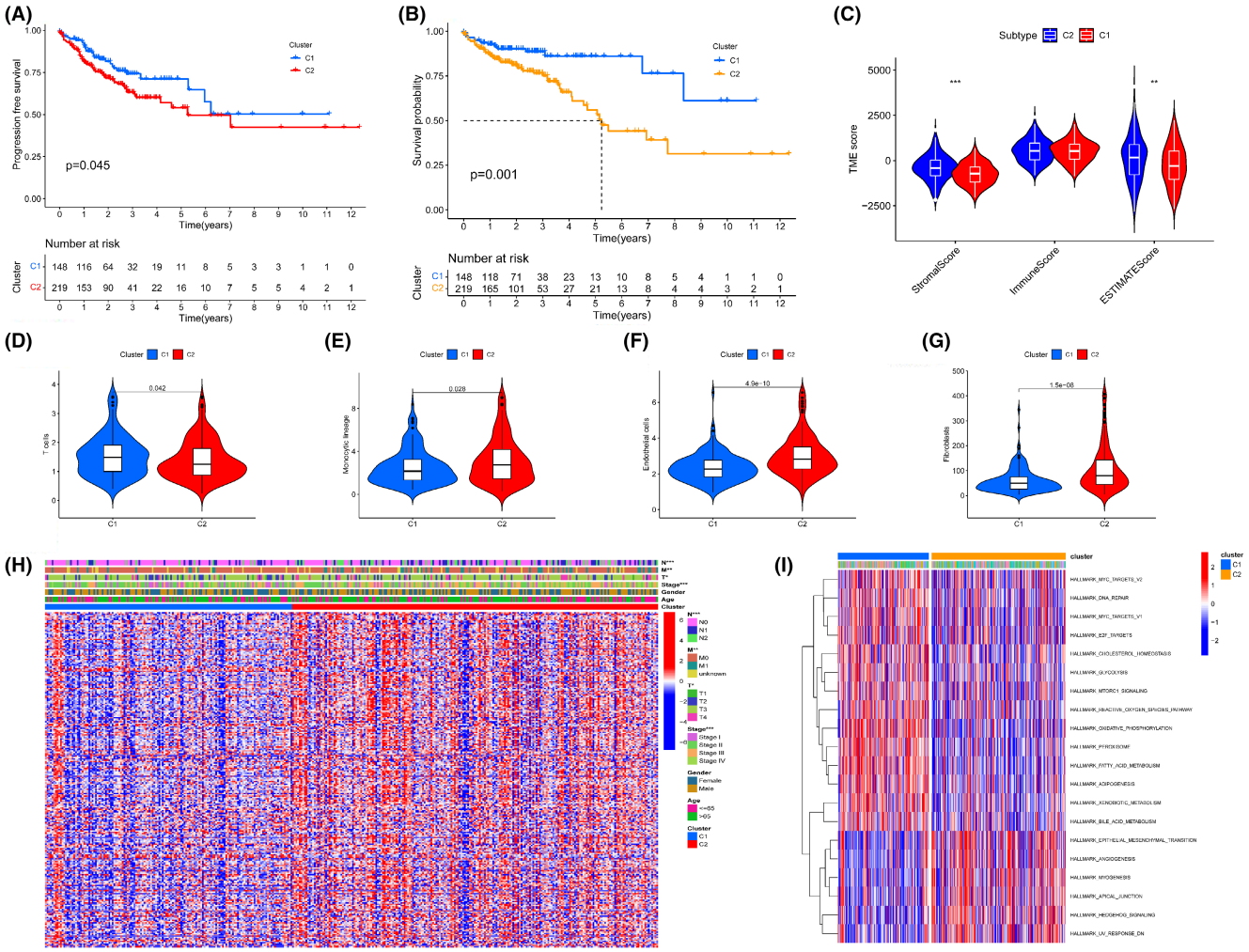

FIGURE 2 The evaluation of the differential degree of clustering. (A, B) PFS and OS curves for the two fatty acid-related clusters based on COAD patients from TCGA cohort. (C) Comparations of stromal, immune, and ESTIMATE scores in tumor tissues between the two groups. (D–G) Comparations between the two groups in immune filtrating cells abundance in tumor tissues. (H) Consensus clustering of DEGs and the clinical characters in the two fatty acid-related clusters of TCGA cohort. (I) Heatmap of gene set variation analysis for microarray and RNA-Seq data (GSVA) between the two groups.

In addition, we then conducted a differential analysis of immune checkpoint genes, HLA genes, pyroptosis-associated genes, and ferroptosis-associated genes. The findings indicated that the high-risk group expressed more HLA and immune checkpoint genes, while the low-risk group expressed more pyroptosis-associated genes and ferroptosis-associated genes (Figure 9A–D).

The CIBERSORT algorithm may be used to determine the relative abundance of different types of cells in mixed cell populations. Therefore, we employed a combination of the normalized COAD patient gene expression matrix and the LM22 feature matrix to assess the 22 human immune cell infiltrations. The total of all predicted immune cell type scores for each sample was equivalent to 1 for each sample. In addition, each sample was screened using the "genfilter" package, with a p-value cutoff of <0.05. We subsequently used "limma" difference analysis of the final output of CIBERSORT. The results indicated an elevated abundance of Macrophages M0, Macrophages M1, and NK cells resting in the high-risk group, while T cells CD4 memory resting, dendritic cells resting, and B cells naïve resting were more abundant in the low-risk group (Figure 10).

3.7 | Relationship between the prognostic signature and drug sensitivity

As chemotherapy is a conventional therapy for COAD, we estimated the response to chemotherapy at half maximum inhibitory concentration (IC50) for each COAD patient with the aid of the R package "pRRophetic" on the Genomics of Tumor Drug Sensitivity (GDSC) website. The findings illustrated that the high-risk group

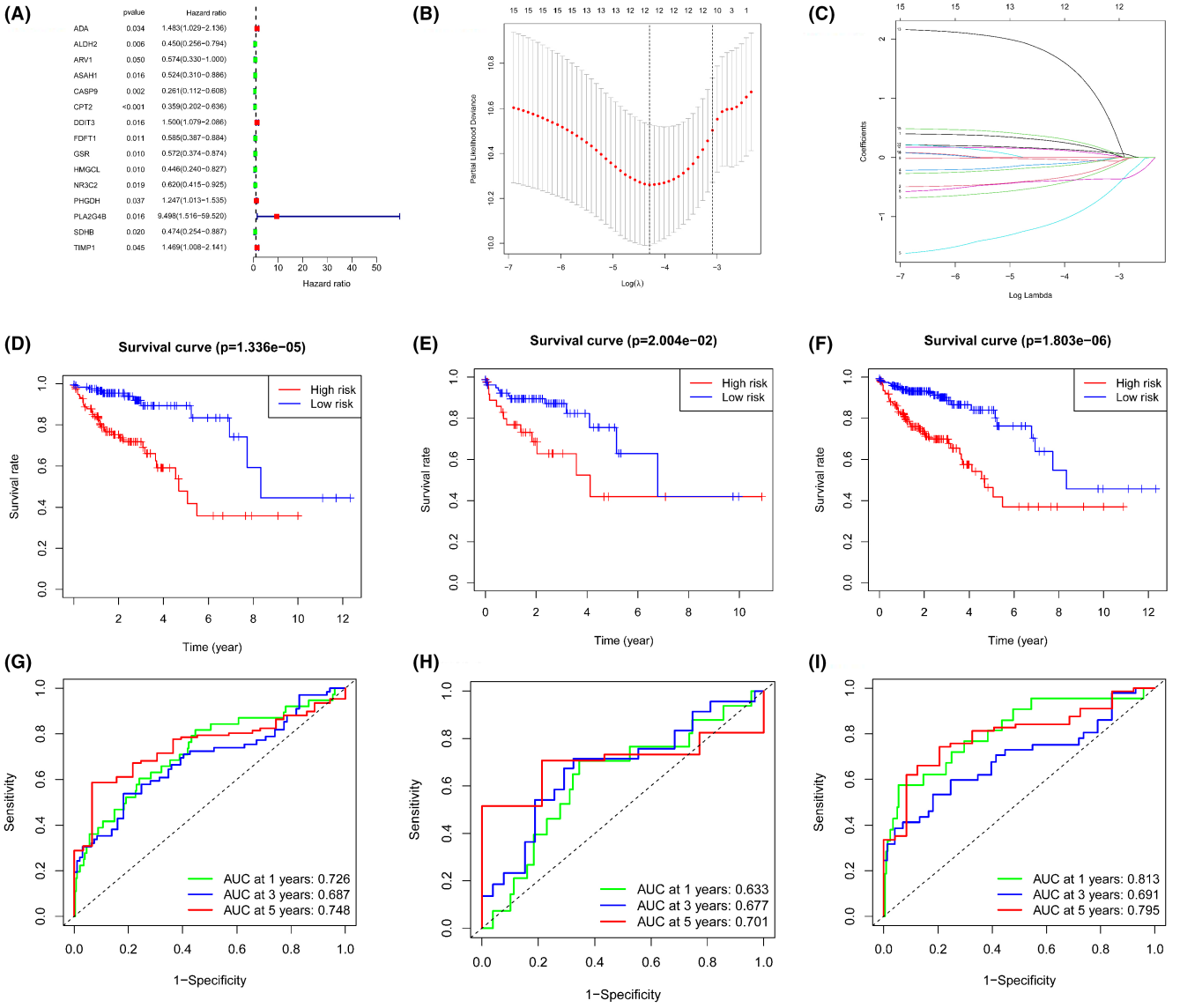

FIGURE 3 Development of the fatty acid metabolism-related risk signature model. (A) In univariate Cox regression, the significance and hazard ratio (95 percent CI) values of OS-related FAMRGs were calculated. (B) The Lasso regression model uncovered the partial probability deviation of variables, where the red dots denotes the partial probability of deviation values, the gray lines denote standard error (SE), and the two vertical dotted lines on the left and right denote optimum values according to minimal and 1-SE criteria, respectively. (C) Lasso coefficient profiles of the 237 fatty acid-related genes in blue modules of the WGCNA. Survival analysis, and ROC analysis of two risk groups of the 12-gene signature in training cohort (D, G), testing cohort (E, H), and all patients (F, I).

exhibited greater sensitivity to VX.680, paclitaxel, gemcitabine, and doxorubicin, and the low-risk group exhibited a higher sensitivity to AKT.inhibitor.VIII (Figure 11A–E). These findings could better guide patients' drug therapy selection.

4 | DISCUSSION

Rectum adenocarcinoma/colon adenocarcinoma (READ/COAD) has been recognized as the most prevalent pathological kind of colorectal cancer (CRC), which is the third commonly occurring and second major contributor of cancer-associated deaths, causing over 800,000 deaths annually all over the world.[19] Young people are more likely to be affected by CRC than older people and children. The deployment of integrative therapies, including surgery and preoperative/postoperative radiation in combination with chemotherapy, has led to a considerable improvement in the 5-year survival rate of CRC patients; nonetheless, invasion and metastasis continue to cause a gloomy prognosis. Furthermore, because of the absence of early specific symptoms, early identification, and follow-up monitoring of COAD remain difficult. Despite the fact that colonoscopy is regarded as the holy grail for diagnosing and monitoring

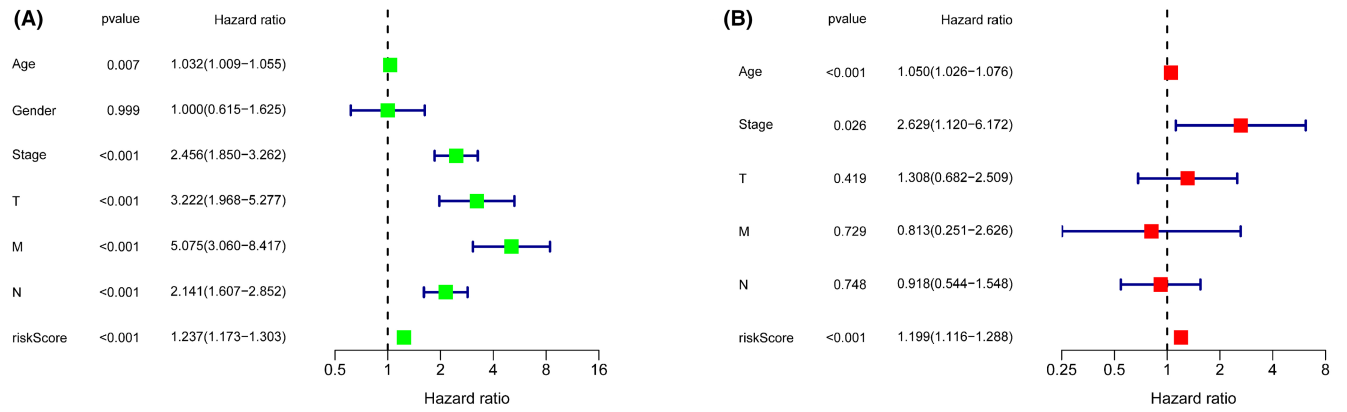

FIGURE 4 Identification of the independence of the developed risk prediction. (A–B) COX regression analysis was used to determine independent prognostic variables.

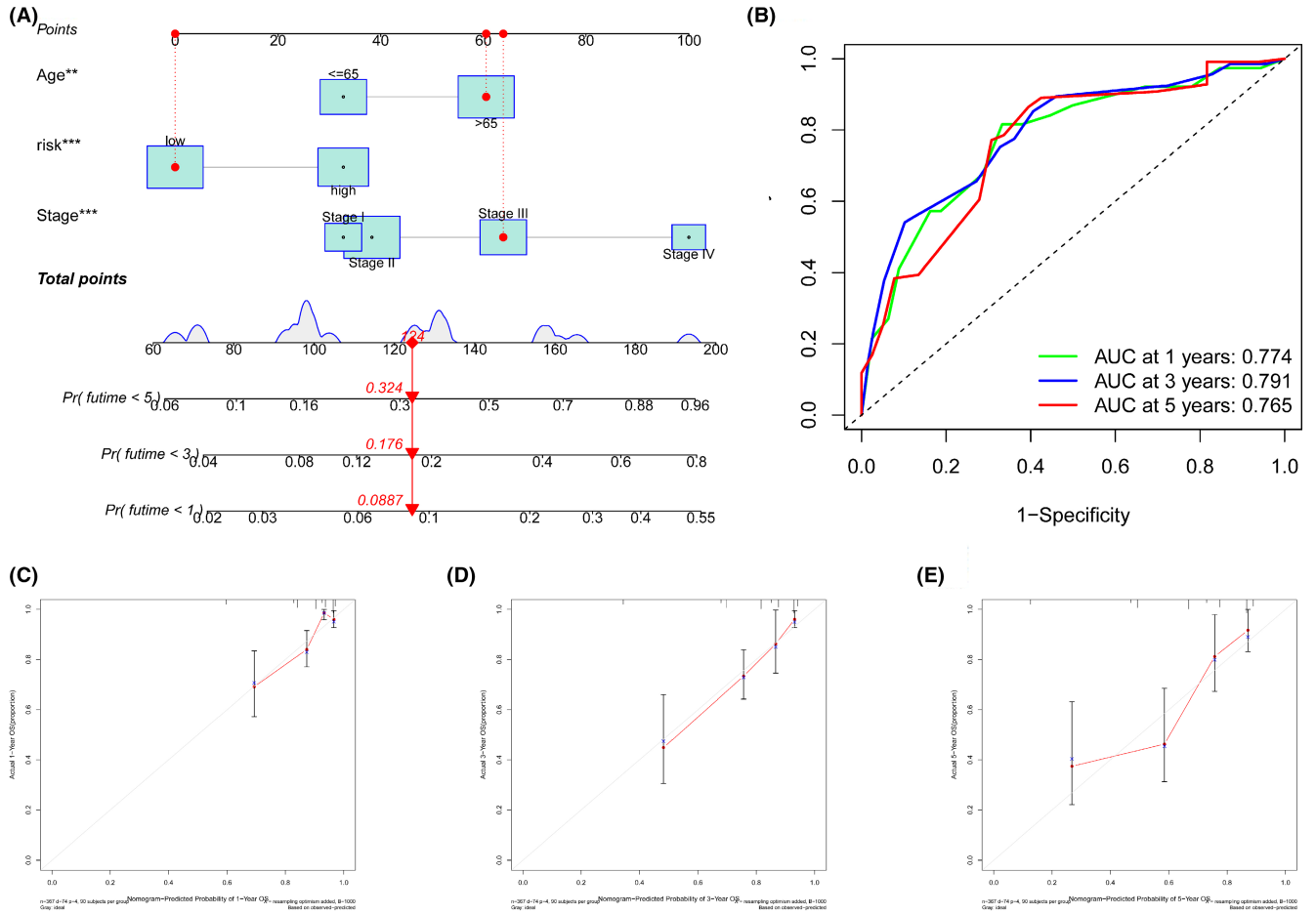

FIGURE 5 Nomogram model development and calibration. (A) Nomogram incorporating clinical and risk factors. (B) The time-dependent ROC curve of the nomogram model. (C–E) Calibration of the nomogram at 1-year, 2-year, and 5-year survival in the TCGA cohort.

COAD, it is an intrusive treatment that frequently leads to distress and does not uncover metastases until they have spread to other organs. As a result, the discovery of tumor-specific biomarkers and risk stratification is critical in determining a patient's prognosis, and this information could be used to promote the development of COAD diagnostic and therapeutic techniques. Furthermore, anticipating the prognosis is vital for therapy decisions as well as the discovery of prognostic biomarkers.

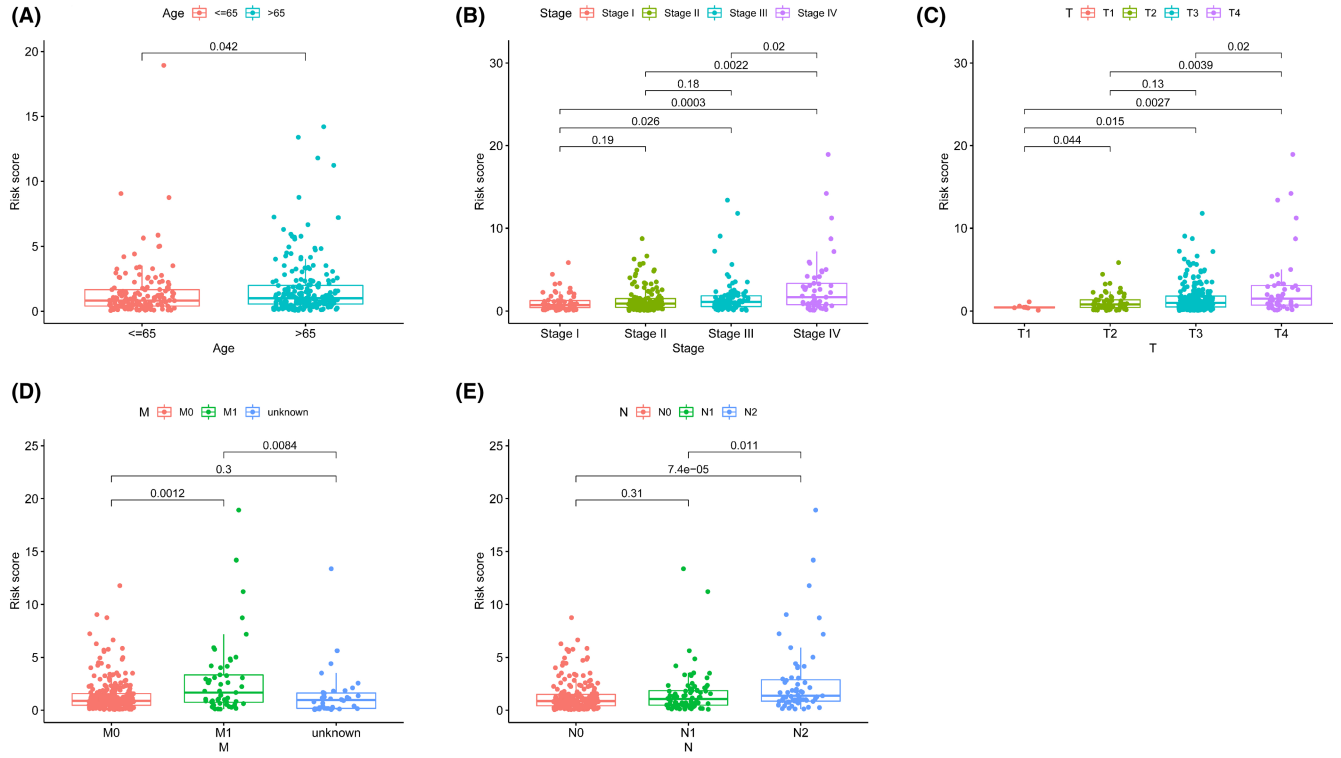

FIGURE 6 Relationship Between the Risk Score and Clinicopathological Characteristics (A) Age. (B) Stage. (C–E) TNM .

CRC etiology is influenced by both genetic history and a variety of adjustable lifestyle and environmental variables.[20] Increasing adiposity, especially abdominal obesity, is associated with a greater risk of CRC incidence.[21] In other words, cancer risk is extremely varied depending on one's diet. At the point where diet-derived signals intersect, white adipose tissue (AT) is now regarded as the major endocrine organ in the body and performs an integral function in maintaining metabolic and immunological homeostasis.[22] Up to date, various research reports have investigated the effect of diet/nutrition in CRC, with findings showing that it may perform both a causative and a preventive role in tumor growth. Apart from being a known risk factor for CRC, increased adiposity is also associated with poorer outcomes.[23] However, the adverse association between obesity and CRC is complicated and has not been completely elucidated so far. A vast spectrum of adipokines and metabolites, with proinflammatory and cancer-causing properties, has been theorized to be produced by AT in this environment, and it has been suggested that this phenomenon may be of critical relevance.[24] Moreover, obesity-related metabolic modifications (such as oxidative stress, endocrine alterations, insulin resistance, impairments in lipid metabolism, and metabolic syndrome) might contribute to the occurrence and progression of CRC.[25–27]

Excessive adiposity and diet may potentially have an impact on the progression of cancer by altering tumor monitoring and modifying the host immunological response. Undoubtedly, white AT is currently acknowledged as the major endocrine organ in which signals from nutrition merge, and it performs a critical function in both metabolic and immunological system homeostasis.[28] In addition, AT, whose polarization profile is dependent on the adipocytes health status, contains a diverse array of immune cells either with proinflammatory (e.g., M1 macrophages, Th1 CD4 and CD8 T lymphocytes, and neutrophils) or anti-inflammatory (e.g., M2 macrophages, and regulatory T [Treg] cells) characteristics.[29,30] In this context, fatty acids (FAs), which are supplied by the diets and processed/released by AT, are becoming more relevant as primary players in this interaction because of their ability to affect both cancer cell growth and the host's immune system. FAs may display a pro- or anti-inflammatory action according to their chemical characteristics, and they have the capacity for modulating host surveillance systems and influencing anticancer reactions by directly regulating both adaptive and innate immunity as well as metabolic homeostasis.[31]

Recently, it has been reported that fatty acid metabolism performs a critical function in the onset and progression of several malignancies.[32] In COAD, the most noticeable morphological feature is a change in the cytoplasm due to the accumulation of glycogen and lipid, indicating that reconfiguration of the fatty acid metabolism is a critical element in the occurrence and progression of the disease.

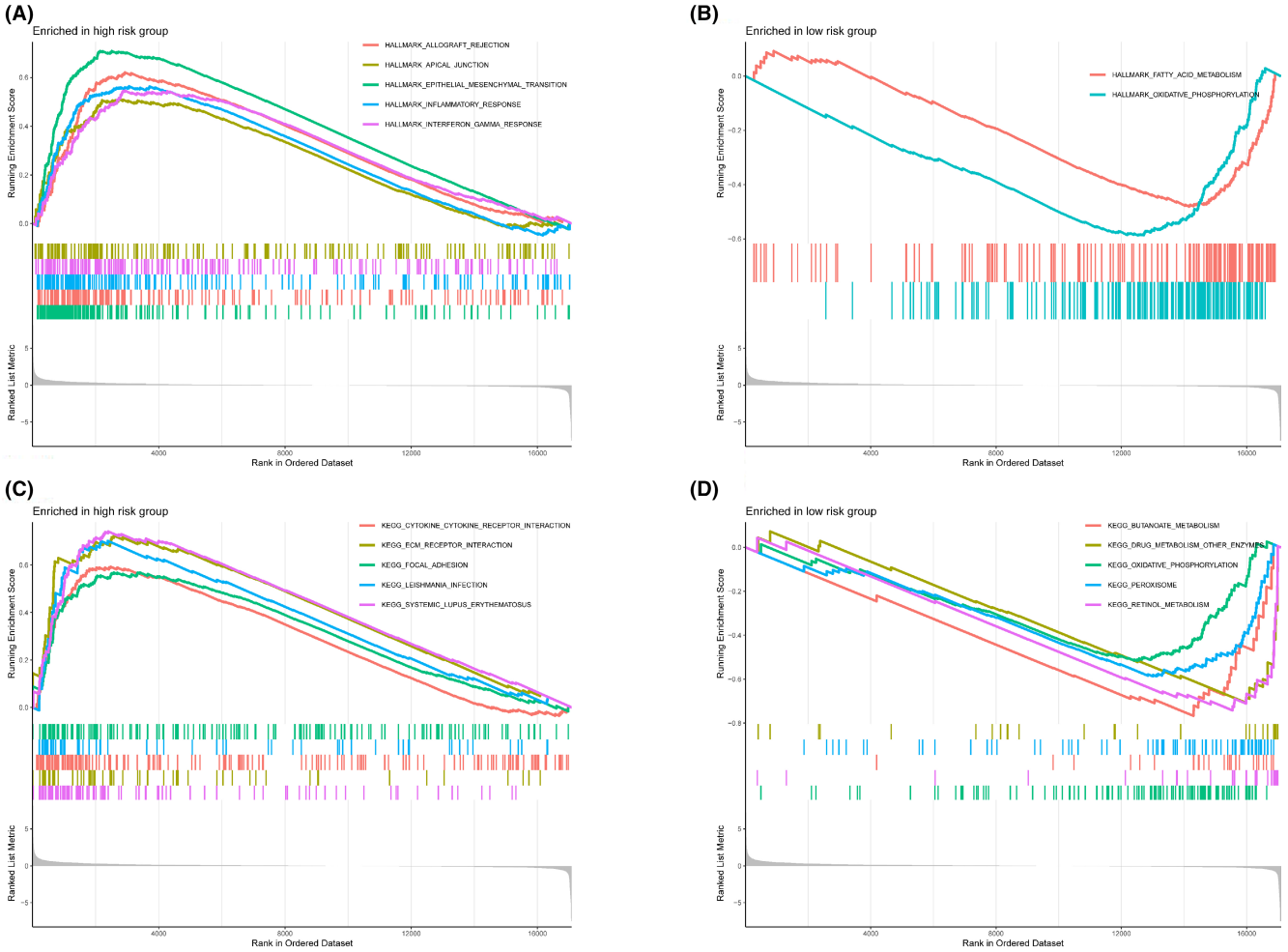

FIGURE 7 Functional enrichment analyses. (A–B) Hallmark gene sets and (C–D) Kyoto Encyclopedia of Genes and Genomes pathways enrichment between high- and low-risk groups in the TCGA-COAD dataset.

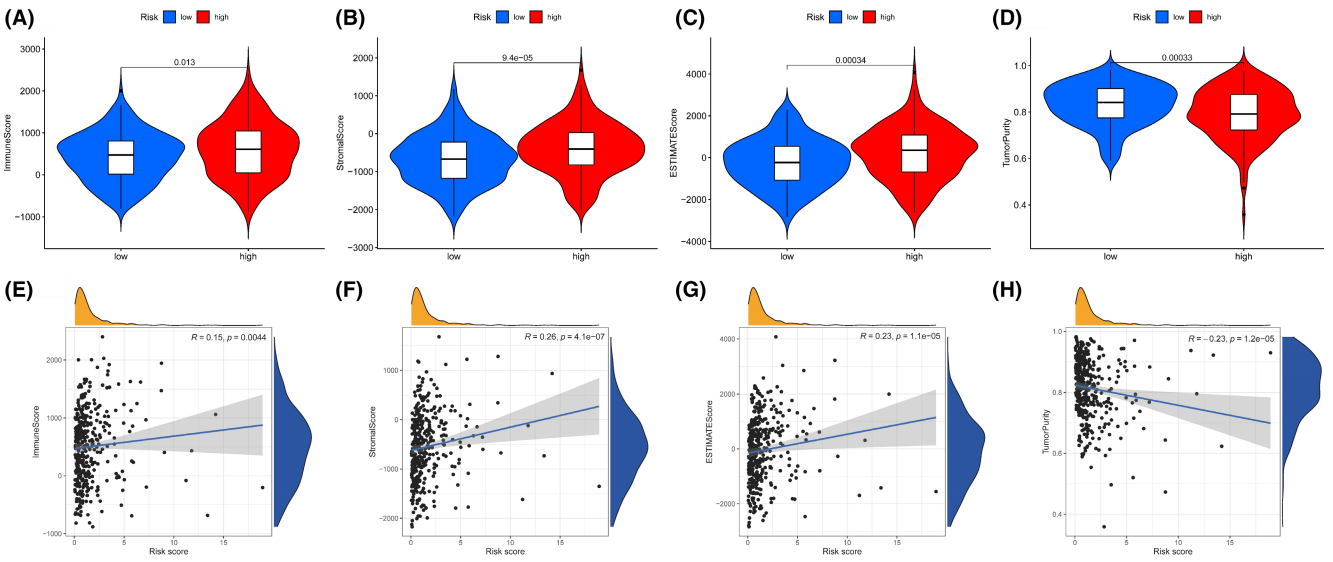

FIGURE 8 Tumor microenvironment analyses. (A–D) High-risk and low-risk groups were compared on tumor purity, stromal, immune, and ESTIMATE scores. (E–H) The relationship between the risk score and stromal score, immune score, ESTIMATE score, and tumor purity in tumor tissues.

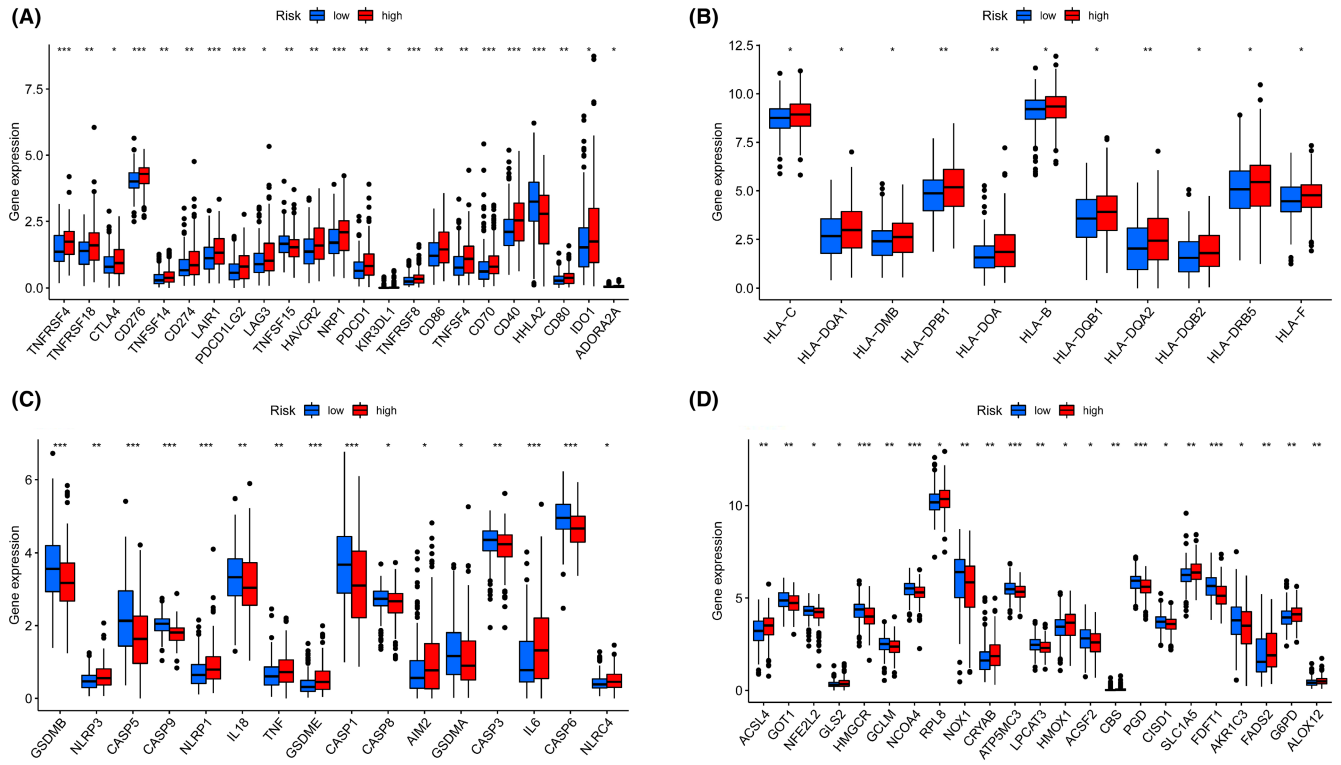

FIGURE 9 Relationships between the risk score with HLA, pyroptosis, ferroptosis, and immune checkpoint genes. Boxplots were utilized to depict the difference of the expressions of Immune checkpoint (A), HLA (B), pyroptosis (C), and ferroptosis (D) genes. *$p < 0.05$, **$p < 0.01$, ***$p < 0.001$.

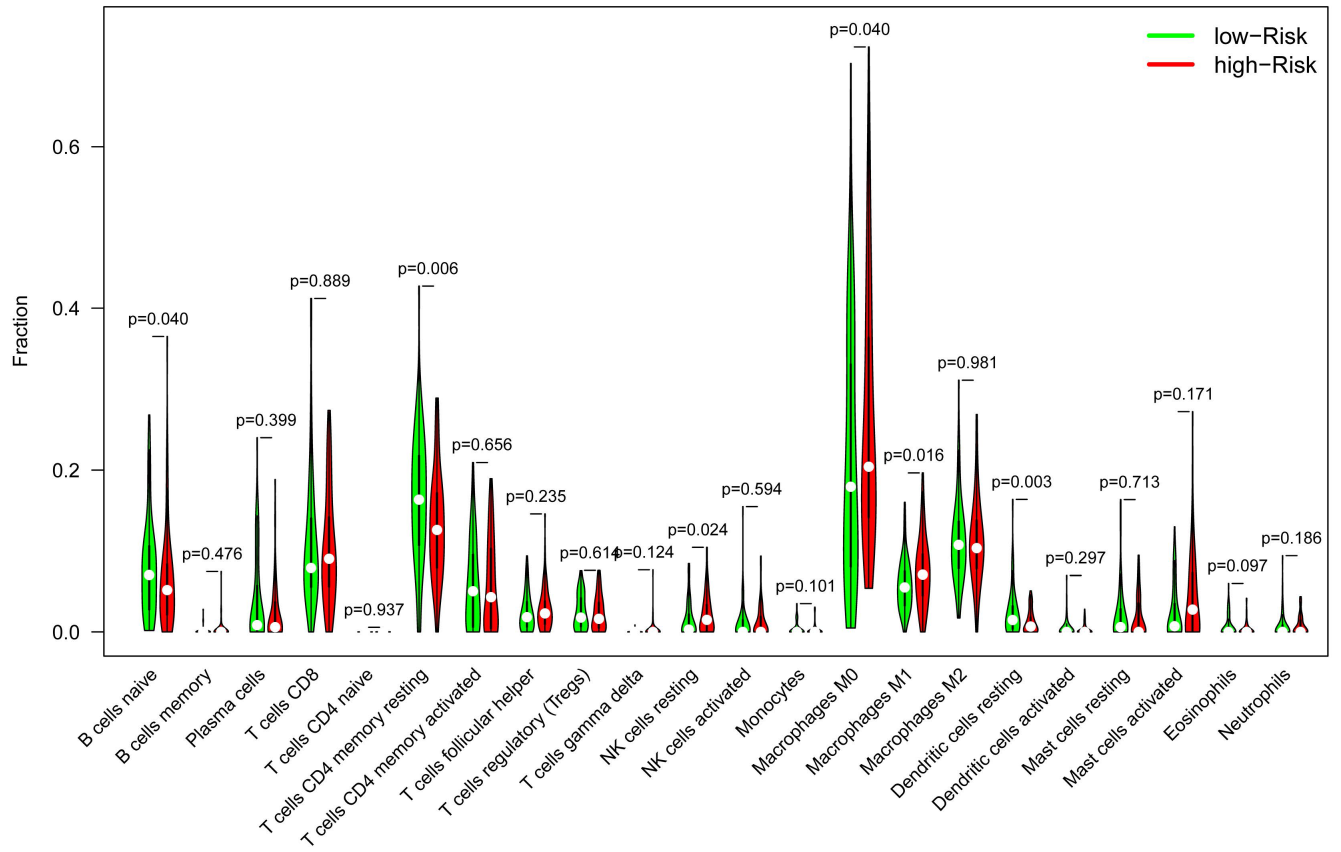

FIGURE 10 Relationship between the risk score and the infiltration levels of immune cells. Immune cell infiltration patterns differ between low- and high-risk patients.

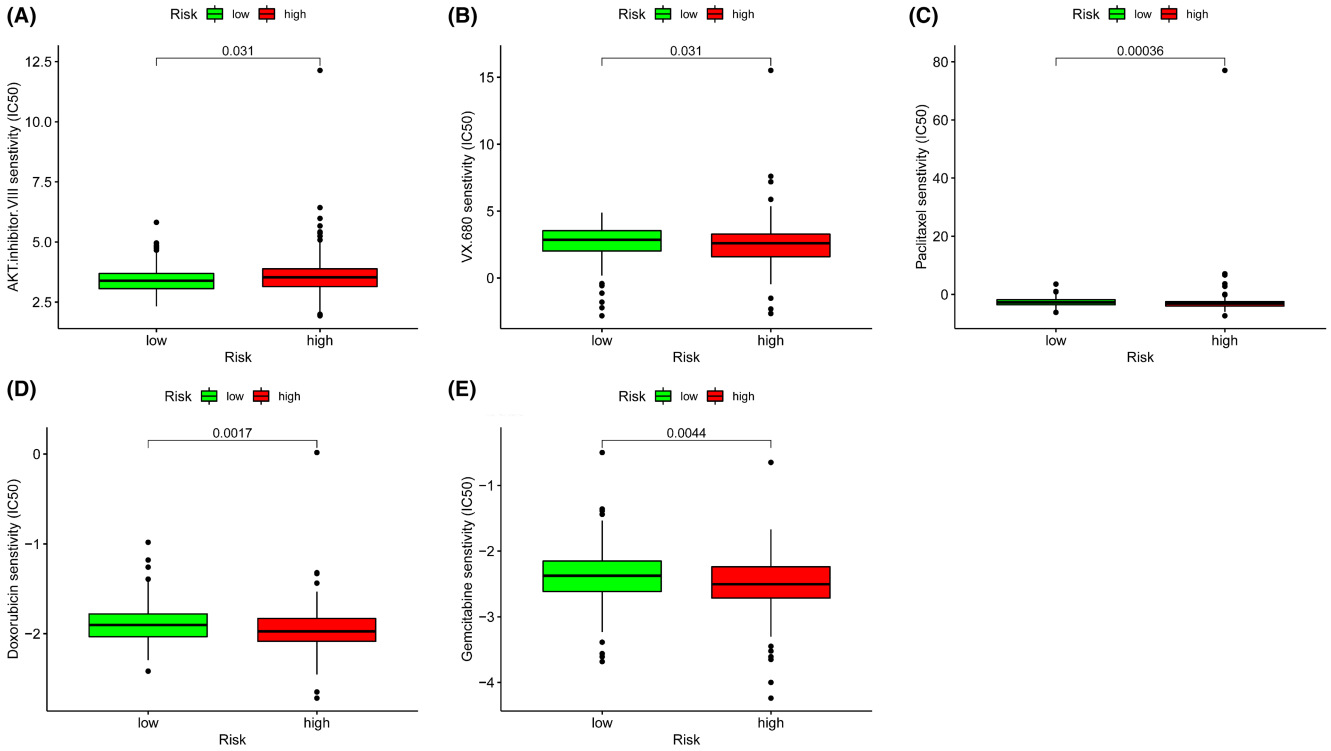

FIGURE 11 Heterogeneous medication resistance. Comparison of the chemotherapeutic responses in high- and low-risk patients with COAD. *$p < 0.05$, **$p < 0.01$, ***$p < 0.001$.

In particular, the tricarboxylic acid (TCA) cycle is downregulated, while the Warburg effect (aerobic glycolysis) is upregulated, which is the most significant change. In the meantime, a study discovered that the Warburg effect seems to be a grade-dependent characteristic regulating the proliferation and viability of COAD cells.[33] As a result, in this research, we retrieved gene expression profiles as well as FAMRG sets from TCGA in order to find the prognostic FAMRG signatures of COAD. Following the LASSO regression, as well as multivariate and univariate Cox regression analyses, 12 FAMRGs (ADA, ALDH2, ARV1, ASAH1, CASP9, CPT2, DDIT3, FDFT1, GSR, PHGDH, PLA2G4B, and TIMP1) were selected to develop a risk signature that can predict clinical prognosis of COAD. ALDH2 is an enzyme involved in ethanol metabolism and acetaldehyde breakdown, such as 4-hydroxykingenal and malondialdehyde, to acetate. In recent years, multiple studies have demonstrated pro-colorectal cancer consequences of ALDH2 activation, which directly regulates metabolic and inflammatory responses.[34] The carnitine palmitoyl transferase system (CPTs) regulates fatty acid β-oxidation. In the outer mitochondrial membrane, CPT1 is situated, while CPT2 is located in the inner mitochondrial membrane. Many studies have linked CPT1 overexpression to tumor development. Furthermore, two recent investigations verified CPT2's significance in colorectal carcinogenesis.[35,36] A precursor enzyme to squalene epoxidase (SQLE) in cholesterol production. Based on their findings, Jiang et al. concluded that FDFT1 is associated with poor prognosis in stage I-III COAD and promotes tumor growth through modifying NAT8 and D-pantethine expression.[37] Inhibiting both FDFT1 and SQLE is a better therapy for stage I-III COAD. The serine synthesis pathway transforms 3-phosphoglycerate to serine via three enzymatic steps, with the NAD-dependent PHGDH as the rate-limiting important enzyme in the first stage of its production pathway. PHGDH is located in the genomic region where recurrent copy number increases are most common in breast and melanoma malignancies.[38,39] To learn more about the "one-carbon" unit and a-ketoglutarate, researchers are studying the relationship between serine synthesis and PHGDH inhibition in cell lines with high PHGDH expression levels.[40] Thus, PHGDH inhibitors as targeted cancer therapy have considerable clinical research value. More research is needed to determine the association between COAD and other proteins expressed by the genes in our risk signature.

To anticipate the 1-, 3-, and 5-year survival of COAD patients, we built a nomogram that integrated risk signatures and clinical parameters. Furthermore, we validated the precision of the nomogram in predicting 1-, 3-, and 5-year survival rates. We categorized 367 patients into high - and low-risk groups using the median risk score as a cutoff value. The Kaplan–Meier curve illustrated that

the low-risk group exhibited a longer OS as opposed to the high-risk group. The AUCs of 1-, 3-, and 5-year OS anticipated by the model were 0.813, 0.691, and 0.795, respectively, verifying the prediction ability of the signature with satisfactory specificity and sensitivity. PCA analysis showed a high degree of discrimination between the high- and low-risk groups. Similar results were obtained by utilizing the same approach for the test dataset. Univariate Cox regression uncovered that risk score and clinical factors such as TNM stage and age were strongly associated with OS, and multifactorial Cox analysis further found that 12-FAPRGs signature was an independent prognostic indicator for COAD, indicating that our signature could be a good complement to conventional pathological staging. Following that, we created a nomogram that included factors including risk score, TNM stage, and age. The model projected AUCs of 0.774, 0.791, and 0.765 for 1-, 3-, and 5-year OS, accordingly.

Recent years have seen the development of a prognostic hallmark for assessing the prognosis of COAD patients. For example, using 11 autophagy genes, Chen et al. developed a predictive signature for predicting the 1-, 3-, and 5-year OS of cancer patients with CRC.[41] Yang et al. developed a prognostic signature for anticipating the 1-, 3-, and 5- year OS using eight ferroptosis-related genes.[42] Additionally, Zhang et al. created a predictive signature based on 6-carbon metabolism and TCA-related mRNAs to predict 1-year OS in COAD.[43] In another study by Song et al., they discovered a signature for evaluating the 3- and 5- year survival probability in CRC patients utilizing seven m6A-modified lncRNAs.[44] One, 3, and 5-year OS AUCs of 0.66, 0.66, and 0.67 were found in a study by Chen et al.[41] However, in research by Yang et al.,[42] the AUCs of OS for the same years were 0.7632, 0.7411, and 0.7581, respectively. Compared to the AUCs in this training set (0.726, 0.687, and 0.748) and pooled set (0.813, 0.691, and 0.795) of the present study, Chen's research had reduced AUCs. Furthermore, For 3-year OS, the AUC in the training and testing sets of the present study (0.808 and 0.819, correspondingly) was greater than that of Shi et al. (0.703 and 0.630). Besides, the calibration plots for the 1-, 3-, and 5-year OS indicated congruence between the predictions made by the nomogram and the actual observations. These findings showed that the current prognostic nomogram is appropriate for assessing the probability of 1-, 3-, and 5-year OS rates in patients with COAD.

There were statistically significant differences in the distributions of risk scores across patients with various grades and TNM stages in both the training and validation sets. Furthermore, a survival assessment of the low- and high-risk groups demonstrated that the high-risk group exhibited a worse prognosis as opposed to the low-risk group. In the meantime, multivariable Cox regression illustrated that the risk score was a prognostic predictor independent of other variables. According to these findings, it was concluded that the fatty acid metabolism-related signature might be utilized as a valid predictor of the prognosis of COAD patients and could be used for the stratification of patients for fatty acid metabolism-focused therapy in the future.

The immunological microenvironment performs an integral function in the progression of cancers. Infiltrating immune cells might function as tumor-promoting or tumor-antagonizing factors. As cancer cells progress in their capacity to block the tumor-antagonizing actions of immune cells and evade immunological monitoring, they are able to promote the growth of cancer tumors. Cancer therapy has seen significant advancements in recent years, with immunotherapy targeting the modulation of immune checkpoints and immune microenvironment showing promising success. Additionally, fatty acid metabolism and immunity have been found to be strongly correlated.[45] Most of the proteins and genes associated with fatty acid metabolism homeostasis are also implicated in the control of fatty acid metabolism fluxes. When exposed to bacterial assaults, cells of the innate immune system, including macrophages, microglia, monocytes as well as lymphocytes, may respond effectively. This result was obtained by carefully managing the fatty acid metabolic fluxes of these cells, which are regulated by FAMRGs. Macrophage is active in fatty acid beta-oxidation and has the largest impact on immunity.[46] According to some noteworthy findings, parenchymal fatty acid beta-oxidation is associated with genes that are usually correlated with the immune system.[47] In this research, we further conducted pathway enrichment analysis. GSEA revealed that distinct pathways involved in the growth of tumors were obviously enriched in the low- and high-risk groups. Nevertheless, drug metabolic processes, as well as fatty acid catabolic processes, were primarily enriched in the low-risk group, while tumor metastasis-related pathways and immune response-related pathways primarily perform a modulatory function in the high-risk group.

We also assessed at the correlation between the risk score model and the immune-related variables. A lower stromal, immune, and ESTIMATE score were seen in the low-risk group, according to these data. In addition, there were more naive B cells, memory CD4+ T cells, and resting dendritic cells infiltrations in low-risk patients, but less resting NK cells, M0 and M1 macrophages infiltrations in high-risk patients. Our results showed that changes in FAMRGs affect the proportion of various B and T cell subtypes and macrophages, resulting in an influence on prognosis. An enhancement in the oxidation catabolism of fatty acid has been shown to trigger the impaired number and function

of natural killer cells, resulting in tumor immune evasion.[48] Therefore, aberrant FAMRG expression could enhance immune evasion by affecting NK cells in the proliferation of COAD. Furthermore, in the present study, the percentage of M0 and M1 macrophages rose in patients in the high-risk group. Macrophages have a role in tumor growth by secreting chemokines and cytokines that have tumorigenic or anti-tumor properties. In addition, Zhou's research discovered that macrophages may engage in the Tregs to enhance COAD progression and medication resistance.[49] It was noticed that the presence of M0 macrophages was substantially associated with recurrence-free survival (RFS) in HCV-HCC.[50] Together with our findings, abnormalities in FAMRGs may impair the activities of macrophages and the interactions between macrophages and T cells to stimulate COAD proliferation.

Furthermore, this research found that the high-risk group exhibited substantially reduced expression of TNFSF15 and HHLA2, and considerably upmodulated expression of CTLA4, CD274, CD276, LAG3, PDCD1, and IDO1. Research has revealed that HHLA2 (a member of the B7 family) was related to cancer progression and immune responses.[51] CD276, known as B7-H3, is a critical component of the immune checkpoint belonging to the CD28 and B7 families. CD276 was discovered to be highly expressed in a variety of tumor cells, where it acts as a suppressor of T-cell activity, leading to a dismal prognosis for cancer patients.[52] IDO1, which is an immuno-modulating enzyme molecule, has been demonstrated to be involved in tumor progression, metastasis, angiogenesis, and tumor immune resistance, according to research findings.[53] The expression level of immune checkpoints is positively correlated with the risk score in a significant way. This indicates that high-risk individuals have a poor prognosis since they are more likely to experience immune evasion and a cancer-promoting immunological milieu. These novel results suggest that exploiting the metabolism-regulated activities in the immune system may be a potential strategy for enhancing anti-tumor effects in the future.

A 17-immune genes-based prognostic signature demonstrated that T cells, natural killer cells, B cells, and macrophages differed between the two groups, and patients in the low-risk group had a higher likelihood of responding to chemotherapy and immunotherapy.[54] The present study demonstrated that a high-risk score was strongly associated with an increased half-IC50 of VX.680, paclitaxel, doxorubicin, and gemcitabine, while a low-risk score was strongly associated with an elevated half-IC50 of AKT inhibitor. Based on these results, our prognostic signature could be used to anticipate the effectiveness of chemotherapy or immunotherapy, which might be useful in clinical practice.

However, despite the fact that the prognostic fatty acid metabolism-related signature displayed a better prediction performance for COAD patients in this research, there are a few drawbacks that need to be resolved. First, because all of the cases were obtained from a publicly accessible database, the possibility of selection bias is nonnegligible. Second, there has been no experimental study undertaken to explore the roles of 12 FAMRGs in COAD. As a result, more research, both in vitro and in vivo, is required to verify the findings of this study.

In conclusion, a predictive risk profile was created based on 12 FAMRGs (ADA, ALDH2, ARV1, ASAH1, CASP9, CPT2, DDIT3, FDFT1, GSR, PHGDH, PLA2G4B, and TIMP1) in COAD, which we examined for their prognostic value. A prognostic nomogram for making predictions of 1-, 3-, and 5-year OS was constructed by integrating a risk signature with clinical data. This nomogram can enhance the clinical outcome predictive performance of the TNM staging system while also serving as a reliable tool for risk evaluation. This study contributes to a better knowledge of fatty acid metabolism status in COAD patients, which will be beneficial to patients undergoing fatty acid metabolism-targeted therapy.

ACKNOWLEDGMENTS

The authors would like to express their gratitude to the TCGA for providing us with free use.

FUNDING INFORMATION

This work was supported by grants from the National Natural Science Foundation of China (No. 81770529 and No. 81900470) and the Postdoctoral Research Foundation of China (No. 2021 M700065).

CONFLICT OF INTEREST

The authors state that there were no commercial or financial relationships that may be considered as a potential conflict of interest during the research.

CREDIT STATEMENT

Le Liu: Project administration; Formal analysis; Resources; Supervision; Funding acquisition; Writing-Original Draft Preparation. Liping Liang: Conceptualization; Data curation; Formal analysis; Methodology; Writing-original draft. Genghui Mai: Conceptualization; Data curation; Investigation; Validation; Supervision. Ye Chen: Project administration; Supervision; Funding acquisition; Writing-review & editing. All of the authors revised the manuscript and approved the final version that was submitted.

DATA AVAILABILITY STATEMENT

The codes used in this study will be deposited in GitHub or a similar repository in the future, and any reasonable requests for information such as analyzed datasets generated could be directed to the corresponding author.

ORCID

Le Liu https://orcid.org/0000-0002-9270-9951
Ye Chen https://orcid.org/0000-0002-7964-7899

REFERENCES

1. Schetter AJ, Leung SY, Sohn JJ, et al. MicroRNA expression profiles associated with prognosis and therapeutic outcome in colon adenocarcinoma. *JAMA*. 2008;299:425-436.
2. Ruan GT, Zhu LC, Gong YZ, et al. The diagnosis and prognosis values of WNT mRNA expression in colon adenocarcinoma. *J Cell Biochem*. 2020;121:3145-3161.
3. Chen EX, Jonker DJ, Loree JM, et al. Effect of combined immune checkpoint inhibition vs best supportive care alone in patients with advanced colorectal cancer: the Canadian cancer trials group CO.26 study. *JAMA Oncol*. 2020;6:831-838.
4. Yaghoubi N, Soltani A, Ghazvini K, Hassanian SM, Hashemy SI. PD-1/PD-L1 blockade as a novel treatment for colorectal cancer. *Biomed Pharmacother*. 2019;110:312-318.
5. Ashizawa M, Okayama H, Aung KTM, et al. Regulation of PD-L1 by MicroRNA in mismatch repair deficient-colorectal cancer. *Gan To Kagaku Ryoho*. 2017;44:889-891.
6. Eisenberg L, Eisenberg-Bord M, Eisenberg-Lerner A, Sagi-Eisenberg R. Metabolic alterations in the tumor microenvironment and their role in oncogenesis. *Cancer Lett*. 2020;484:65-71.
7. Pavlova NN, Thompson CB. The emerging hallmarks of cancer metabolism. *Cell Metab*. 2016;23:27-47.
8. La Vecchia S, Sebastian C. Metabolic pathways regulating colorectal cancer initiation and progression. *Semin Cell Dev Biol*. 2020;98:63-70.
9. Wang Y, Yang Y, Wang X, Jin T, Zhu G, Lin Z. Ezrin as a prognostic indicator regulates colon adenocarinoma progression through glycolysis. *J Gastroenterol Hepatol*. 2021;36:710-720.
10. Pakiet A, Kobiela J, Stepnowski P, Sledzinski T, Mika A. Changes in lipids composition and metabolism in colorectal cancer: a review. *Lipids Health Dis*. 2019;18:29.
11. Hofmanova J, Slavik J, Ciganek M, et al. Complex alterations of fatty acid metabolism and phospholipidome uncovered in isolated colon cancer epithelial cells. *Int J Mol Sci*. 2021;22(13):6650.
12. Li Q, Cao L, Tian Y, et al. Butyrate suppresses the proliferation of colorectal cancer cells via targeting pyruvate kinase M2 and metabolic reprogramming. *Mol Cell Proteomics*. 2018;17:1531-1545.
13. Kesh K, Garrido VT, Dosch A, et al. Stroma secreted IL6 selects for "stem-like" population and alters pancreatic tumor microenvironment by reprogramming metabolic pathways. *Cell Death Dis*. 2020;11:967.
14. Shang RZ, Qu SB, Wang DS. Reprogramming of glucose metabolism in hepatocellular carcinoma: progress and prospects. *World J Gastroenterol*. 2016;22:9933-9943.
15. de Carvalho C, Caramujo MJ. The various roles of fatty acids. *Molecules*. 2018;23(10):2583.
16. Wang YN, Zeng ZL, Lu J, et al. CPT1A-mediated fatty acid oxidation promotes colorectal cancer cell metastasis by inhibiting anoikis. *Oncogene*. 2018;37:6025-6040.
17. Langfelder P, Horvath S. WGCNA: an R package for weighted correlation network analysis. *BMC Bioinformatics*. 2008;9:559.
18. Yang W, Soares J, Greninger P, et al. Genomics of drug sensitivity in cancer (GDSC): a resource for therapeutic biomarker discovery in cancer cells. *Nucleic Acids Res*. 2013;41:D955-D961.
19. Dekker E, Tanis PJ, Vleugels J, et al. Colorectal cancer. *Lancet*. 2019;394:1467-1480.
20. Keum N, Giovannucci E. Global burden of colorectal cancer: emerging trends, risk factors and prevention strategies. *Nat Rev Gastroenterol Hepatol*. 2019;16:713-732.
21. Bardou M, Barkun AN, Martel M. Obesity and colorectal cancer. *Gut*. 2013;62:933-947.
22. Biondo LA, Teixeira A, Silveira LS, et al. Tributyrin in inflammation: does white adipose tissue affect colorectal cancer? *Nutrients*. 2019;11:110.
23. Bull CJ, Bell JA, Murphy N, et al. Adiposity, metabolites, and colorectal cancer risk: Mendelian randomization study. *BMC Med*. 2020;18:396.
24. Riondino S, Roselli M, Palmirotta R, Della-Morte D, Ferroni P, Guadagni F. Obesity and colorectal cancer: role of adipokines in tumor initiation and progression. *World J Gastroenterol*. 2014;20:5177-5190.
25. Wu Z, Zuo M, Zeng L, et al. OMA1 reprograms metabolism under hypoxia to promote colorectal cancer development. *EMBO Rep*. 2021;22:e50827.
26. Satoh K, Yachida S, Sugimoto M, et al. Global metabolic reprogramming of colorectal cancer occurs at adenoma stage and is induced by MYC. *Proc Natl Acad Sci USA*. 2017;114:E7697-E7706.
27. Tang J, Yan T, Bao Y, et al. LncRNA GLCC1 promotes colorectal carcinogenesis and glucose metabolism by stabilizing c-Myc. *Nat Commun*. 2019;10:3499.
28. Clemente-Postigo M, Tinahones A, El BR, et al. The role of autophagy in white adipose tissue function: implications for metabolic health. *Metabolites*. 2020;10:179.
29. Han SJ, Glatman ZA, Andrade-Oliveira V, et al. White adipose tissue is a reservoir for memory T cells and promotes protective memory responses to infection. *Immunity*. 2017;47:1154-1168.
30. Cox AR, Chernis N, Masschelin PM, Hartig SM. Immune cells gate white adipose tissue expansion. *Endocrinology*. 2019;160:1645-1658.
31. Veglia F, Tyurin VA, Blasi M, et al. Fatty acid transport protein 2 reprograms neutrophils in cancer. *Nature*. 2019;569:73-78.
32. Koundouros N, Poulogiannis G. Reprogramming of fatty acid metabolism in cancer. *Br J Cancer*. 2020;122:4-22.
33. Dai W, Meng X, Mo S, et al. FOXE1 represses cell proliferation and Warburg effect by inhibiting HK2 in colorectal cancer. *Cell Commun Signal*. 2020;18:7.
34. Zhang H, Xia Y, Wang F, et al. Aldehyde dehydrogenase 2 mediates alcohol-induced colorectal cancer immune escape through stabilizing PD-L1 expression. *Adv Sci (Weinh)*. 2021;8:2003404.

35. Li H, Chen J, Liu J, et al. CPT2 downregulation triggers stemness and oxaliplatin resistance in colorectal cancer via activating the ROS/Wnt/beta-catenin-induced glycolytic metabolism. *Exp Cell Res*. 2021;409:112892.
36. Liu F, Li X, Yan H, et al. Downregulation of CPT2 promotes proliferation and inhibits apoptosis through p53 pathway in colorectal cancer. *Cell Signal*. 2022;92:110267.
37. Jiang H, Tang E, Chen Y, et al. Squalene synthase predicts poor prognosis in stage I-III colon adenocarcinoma and synergizes squalene epoxidase to promote tumor progression. *Cancer Sci*. 2022;113:971-985.
38. Possemato R, Marks KM, Shaul YD, et al. Functional genomics reveal that the serine synthesis pathway is essential in breast cancer. *Nature*. 2011;476:346-350.
39. Mullarky E, Mattaini KR, Vander HM, et al. PHGDH amplification and altered glucose metabolism in human melanoma. *Pigment Cell Melanoma Res*. 2011;24:1112-1115.
40. Zhang Y, Yu H, Zhang J, et al. Cul4A-DDB1-mediated monoubiquitination of phosphoglycerate dehydrogenase promotes colorectal cancer metastasis via increased S-adenosylmethionine. *J Clin Invest*. 2021;131:e146187.
41. Chen S, Wang Y, Wang B, et al. A signature based on 11 autophagy genes for prognosis prediction of colorectal cancer. *Plos One*. 2021;16:e258741.
42. Yang C, Huang S, Cao F, Zheng Y. Role of ferroptosis-related genes in prognostic prediction and tumor immune microenvironment in colorectal carcinoma. *PeerJ*. 2021;9:e11745.
43. Zhang Z, Zhu H, Li Q, et al. Gene expression profiling of tricarboxylic acid cycle and one carbon metabolism related genes for prognostic risk signature of colon carcinoma. *Front Genet*. 2021;12:647152.
44. Song W, Ren J, Yuan W, Xiang R, Ge Y, Fu T. N6-Methyladenosine-related lncRNA signature predicts the overall survival of colorectal cancer patients. *Genes (Basel)*. 2021;12:1375.
45. Lochner M, Berod L, Sparwasser T. Fatty acid metabolism in the regulation of T cell function. *Trends Immunol*. 2015;36:81-91.
46. Zhang Q, Wang H, Mao C, et al. Fatty acid oxidation contributes to IL-1beta secretion in M2 macrophages and promotes macrophage-mediated tumor cell migration. *Mol Immunol*. 2018;94:27-35.
47. Patsoukis N, Bardhan K, Chatterjee P, et al. PD-1 alters T-cell metabolic reprogramming by inhibiting glycolysis and promoting lipolysis and fatty acid oxidation. *Nat Commun*. 2015;6:6692.
48. Hu X, Jia X, Xu C, et al. Downregulation of NK cell activities in apolipoprotein C-III-induced hyperlipidemia resulting from lipid-induced metabolic reprogramming and crosstalk with lipid-laden dendritic cells. *Metabolism*. 2021;120:154800.
49. Zhou S, Tu J, Ding S, et al. High expression of angiopoietin-like protein 4 in advanced colorectal cancer and its association with regulatory T cells and M2 macrophages. *Pathol Oncol Res*. 2020;26:1269-1278.
50. Hsiao YW, Chiu LT, Chen CH, Shih WL, Lu TP. Tumor-infiltrating leukocyte composition and prognostic power in hepatitis B- and hepatitis C-related hepatocellular carcinomas. *Genes (Basel)*. 2019;10:630.
51. Sun W, Li S, Tang G, et al. HHLA2 deficiency inhibits non-small cell lung cancer progression and THP-1 macrophage M2 polarization. *Cancer Med*. 2021;10:5256-5269.
52. Picarda E, Ohaegbulam KC, Zang X. Molecular pathways: targeting B7-H3 (CD276) for human cancer immunotherapy. *Clin Cancer Res*. 2016;22:3425-3431.
53. Xiang Z, Li J, Song S, et al. A positive feedback between IDO1 metabolite and COL12A1 via MAPK pathway to promote gastric cancer metastasis. *J Exp Clin Cancer Res*. 2019;38:314.
54. Zhang Z, Li J, He T, Ding J. Bioinformatics identified 17 immune genes as prognostic biomarkers for breast cancer: application study based on artificial intelligence algorithms. *Front Oncol*. 2020;10:330.

SUPPORTING INFORMATION

Additional supporting information may be found in the online version of the article at the publisher's website.

How to cite this article: Liu L, Liang L, Mai G, Chen Y. A novel fatty acid metabolism-related gene signature predicts the prognosis, tumor immune properties, and immunotherapy response of colon adenocarcinoma patients. *FASEB BioAdvances*. 2022;4(9):585-601. doi: 10.1096/fba.2022-00017